

## Experimental evaluation of acceleration correlations for locally isotropic turbulence

Reginald J. Hill

NOAA/ERL/Environmental Technology Laboratory, 325 Broadway, Boulder, Colorado 80303-3328

S. T. Thoroddsen

University of Illinois at Urbana-Champaign, Department of Theoretical and Applied Mechanics, 104 South Wright Street, Urbana, Illinois 61801-2935

(Received 3 September 1996)

The two-point correlation of the fluid-particle acceleration is the sum of the pressure gradient and viscous force correlations. The pressure-gradient correlation is related to the fourth-order velocity structure function. The acceleration correlation caused by viscous forces is formulated in terms of the third-order velocity structure function. Velocity data from grid-generated turbulence in a wind tunnel are used to evaluate these quantities. The evaluated relationships require only the Navier-Stokes equation, incompressibility, local homogeneity, and local isotropy. The relationships are valid for any Reynolds number. For the moderate Reynolds number of the wind-tunnel turbulence, the acceleration correlation is roughly three times larger than if it is evaluated on the basis of the assumption that velocities at several points are joint Gaussian random variables. The correlation of components of acceleration parallel to the separation vector of the two points is negative near its minimum at spacings close to 17 times the microscale. Its value near this minimum implies that fluid particles at those spacings have typical relative accelerations of one-half that of gravity in the directions toward and away from one another. For large Reynolds numbers, the two-point correlation of acceleration is dominated by the two-point correlation of the pressure gradient. The data verify that the acceleration correlation caused by viscous forces is much smaller than that caused by the pressure gradient. [S1063-651X(97)12402-3]

PACS number(s): 47.10.+g, 47.27.Gs, 47.27.Jv, 47.27.Ak

### I. INTRODUCTION

For brevity, the Navier-Stokes equation, incompressibility, local homogeneity, and local isotropy are referred to as the postulates. On the basis of these postulates alone, formulas are given for the two-point correlation of fluid-particle acceleration in terms of velocity structure functions. These formulas are evaluated using data from grid-generated turbulence in a wind tunnel. Conditions for the accuracy of local isotropy have recently been systematically studied by means of experiment [1] and numerical simulation [2].

The time derivative of the velocity  $u_i$  following the motion of a fluid particle is the Lagrangian acceleration denoted by  $Du_i/Dt$ , where  $t$  is time and subscript  $i$  denotes the component of velocity. Fluid-particle acceleration is another name for Lagrangian acceleration. The Navier-Stokes equation relates the Lagrangian acceleration to the accelerations caused by the pressure gradient and viscous forces [3,4],

$$\frac{Du_i}{Dt} = \partial_t u_i + u_k \partial_k u_i = -\frac{1}{\rho} P + \nu \nabla^2 u_i, \quad (1)$$

where  $\partial_t$  and  $\partial_i$  denote partial differentiation with respect to time and spatial position component  $x_i$ , respectively, and  $\nabla^2 = \partial_k \partial_k$  is the Laplacian operator. Repeated Roman indices imply summation. From Eq. (1), it follows that the two-point spatial correlation of Lagrangian acceleration is given by [3,4]

$$\left\langle \left( \frac{Du_i}{Dt} \right) \left( \frac{Du_j}{Dt} \right)' \right\rangle = \frac{1}{\rho^2} \langle \partial_i P \partial_j P' \rangle + \nu^2 \langle \nabla^2 u_i \nabla'^2 u_j' \rangle, \quad (2)$$

where primed and unprimed quantities are evaluated at points  $\vec{x}'$  and  $\vec{x}$ , respectively. Angle brackets denote an average. Pressure is denoted by  $P$ , density by  $\rho$ , and the kinematic viscosity by  $\nu$ . The cross term involving the correlation of pressure gradient with velocity vanishes on the basis of local isotropy [3,4], and is therefore omitted from Eq. (2). The pressure-gradient correlation in Eq. (2) (the first term on the right-hand side) has zero curl, and the viscous acceleration correlation in Eq. (2) has zero divergence. Thus, these two terms are the potential and solenoidal contributions to the acceleration correlation.

For locally homogeneous turbulence, the statistical tensors depend on the separation vector  $\vec{r} = \vec{x} - \vec{x}'$ , and for locally isotropic turbulence, the tensors' associated scalar functions depend only on the spacing  $r = |\vec{r}|$ . The preferred coordinate system is the Cartesian coordinate system having its 1-axis aligned along the separation vector  $\vec{r}$ . Transverse components are denoted by Greek subscripts such as  $\alpha$ ,  $\beta$ , and  $\gamma$ ; that is,  $\alpha$ ,  $\beta$ , and  $\gamma$  are 2 and 3, and they can be equal unless otherwise specified. No summation is implied by repeated Greek subscripts. For our purposes, the Reynolds number is defined by  $Re = l_T \langle u_1^2 \rangle^{1/2} / \nu$ , where Taylor's scale is defined by  $l_T = \langle u_1^2 \rangle / [(\partial_t u_1)^2]^{1/2}$ . The traditional notation  $\lambda$  for Taylor's scale and its use as a subscript on  $Re$  is avoided because Greek subscripts have another meaning here.

The correlation of fluid-particle acceleration has been studied by Batchelor [5] and Obukhov and Yaglom [3,6]. They showed that for large Reynolds numbers the contribution of the viscous acceleration is very small compared with that of the pressure gradient. Batchelor [5] gave the quantitative estimate that the correlation of the viscous term contributes only 2% of the acceleration correlation at zero spac-

ing and for large Re (a Reynolds number of 200 is large for his purposes; cf. Fig. 3 of Ref. [5]); his estimate was based on the assumption that velocities at two points have the joint Gaussian probability distribution. Deviations of pressure statistics from the formulas based on the joint Gaussian assumption have been obtained from numerical simulation of turbulence for low Re [7,8]. On the basis of the postulates (but without use of the joint Gaussian assumption), the pressure structure function and pressure-gradient correlation have recently been related to the fourth-order velocity structure function [9]. It was thereby shown that the estimates of the pressure-gradient correlation based on the joint Gaussian assumption were underestimates, and that the underestimate worsens with increasing Re such that for values of Re typically observed in the atmospheric surface layer (Re in the range of several thousands), the underestimate was about a factor of 4 [9]. For the data shown here, Re=208, and the underestimate from the joint Gaussian assumption is shown to be about a factor of 3. Obukhov and Yaglom [3] showed that for increasing  $r$  the viscous acceleration correlation becomes progressively smaller relative to the pressure-gradient acceleration correlation. Therefore, the viscous acceleration correlation is only about one-third (for Re=208) of Batchelor's [5] estimate of 2% of the total acceleration correlation at  $r=0$  and becomes progressively smaller, relative to the total, with increasing  $r$  and Re.

Referring to Eq. (1), Monin and Yaglom [4] named the term  $\partial_t u_i$  the "local acceleration" and named  $u_k \partial_k u_i$  the "inertial acceleration." Lin [10] studied the auto- and cross-covariances of all four acceleration terms in Eq. (1). He found that the mean-squared pressure gradient was smaller than the mean-squared inertial acceleration by a factor of order  $\text{Re}^{-1}$  and that the mean-squared viscous acceleration was even smaller. Therefore, the local and inertial accelerations are much larger than the right-hand side of Eq. (1); they nearly cancel each other, and they cancel more completely as Re increases. The total nonlinear term in the Navier-Stokes equation, i.e., the sum of inertial and pressure-gradient accelerations, is therefore dominated by the inertial acceleration. The total nonlinear term has been studied by means of numerical simulation of turbulence [11], and its deviations from the predictions of the joint Gaussian assumption were given in Ref. [11].

Münch and Wheelon [12] used the Navier-Stokes equation to study the Eulerian velocity correlation time. In so doing, they demonstrated that advection of small-scale structure by the large-scale motion dominates the mean-squared local acceleration. This effect has more recently been called "random sweeping." Tennekes [13] used random sweeping to obtain that the mean-squared Lagrangian acceleration is  $\text{Re}^{-1}$  times the mean-squared local acceleration; this is equivalent to Lin's [10] result. Tennekes [13] expressed the random sweeping hypothesis in his first equation, which is  $\partial_t u_i + u_k \partial_k u_i = 0$ ; that is, the right-hand side of Eq. (1) is neglected. Thus, the pressure-gradient and viscous accelerations produce deviations from the random sweeping hypothesis. The importance of pressure-gradient and viscous accelerations to Taylor's hypothesis of frozen flow has been assessed in Refs. [10] and [14].

The pressure structure function is needed in subsequent sections; it is defined by

$$D_P(\vec{r}) \equiv \frac{1}{\rho^2} \langle (P - P')^2 \rangle. \quad (3)$$

The following second-, third-, and fourth-order velocity structure functions are also needed:

$$D_{ij}(\vec{r}) \equiv \langle (u_i - u'_i)(u_j - u'_j) \rangle, \quad (4a)$$

$$D_{ijk}(\vec{r}) \equiv \langle (u_i - u'_i)(u_j - u'_j)(u_k - u'_k) \rangle, \quad (4b)$$

$$D_{ijkl}(\vec{r}) \equiv \langle (u_i - u'_i)(u_j - u'_j)(u_k - u'_k)(u_l - u'_l) \rangle. \quad (4c)$$

These tensors are symmetric under interchange of every pair of indices. Assuming local isotropy, these tensors [Eqs. (4a)–(4c)] obey the specific "isotropic" formulas (13.69), (13.80), and (13.81) of Monin and Yaglom [4]. For instance, a general locally isotropic second-order tensor  $T_{ij}(\vec{r})$  is given by [4]

$$T_{ij}(\vec{r}) = [T_{11}(r) - T_{\gamma\gamma}(r)] \frac{r_i r_j}{r^2} + T_{\gamma\gamma}(r) \delta_{ij}, \quad (5)$$

where  $T_{11}(r)$  and  $T_{\gamma\gamma}(r)$  are the longitudinal and transverse components of the tensor, respectively, and  $\delta_{ij}$  is the Kronecker delta. For locally isotropic turbulence, the Lagrangian acceleration correlation and its two contributions in Eq. (2) obey Eq. (5), as does  $D_{ij}(\vec{r})$ . Also,  $D_{ijk}(\vec{r})$  can be expressed in terms of its nonzero components  $D_{111}(r)$  and  $D_{1\gamma\gamma}(r)$ , which are related by the incompressibility condition [4]

$$D_{1\gamma\gamma}(r) = \frac{1}{6} [r D_{111}(r)]^{(1)}. \quad (6)$$

The superscript in parentheses indicates the order of differentiation with respect to  $r$ . Also,  $D_{ijkl}(\vec{r})$  can be expressed in terms of its nonzero components  $D_{1111}(r)$ ,  $D_{\beta\beta\beta\beta}(r)$ , and  $D_{11\gamma\gamma}(r)$ , and the other nonzero components,  $D_{\kappa\kappa\gamma\gamma}(r)$  with  $\kappa \neq \gamma$ , are related to  $D_{\beta\beta\beta\beta}(r)$  by the isotropy condition  $3D_{\kappa\kappa\gamma\gamma}(r) = D_{\beta\beta\beta\beta}(r)$  [4].

## II. ACCELERATION CORRELATION BY THE PRESSURE GRADIENT

The pressure-gradient contribution to the Lagrangian acceleration correlation in Eq. (2) can be expressed as [3]

$$A_{ij}(\vec{r}) \equiv \frac{1}{\rho^2} \langle \partial_i P \partial_j' P' \rangle = \frac{1}{2} D_P(r) |_{ij}. \quad (7)$$

The subscript vertical bar followed by indices indicates differentiation with respect to the components of  $\vec{r}$ . On the basis of the postulates, the relationship between  $D_P(r)$  and  $D_{ijkl}(\vec{r})$  gives [9]

$$\begin{aligned}
A_{\gamma\gamma}(r) &= \frac{1}{2r} D_P^{(1)}(r) \\
&= -\frac{1}{6r} D_{1111}^{(1)}(r) - \frac{2}{3r^2} [D_{1111}(r) - 3D_{11\alpha\alpha}(r)] \\
&\quad + \frac{4}{3} \int_r^\infty y^{-3} [D_{1111}(r) + D_{\beta\beta\beta\beta}(r) \\
&\quad - 6D_{11\alpha\alpha}(r)] dy, \tag{8a}
\end{aligned}$$

$$\begin{aligned}
A_{11}(r) &= \frac{1}{2} D_P^{(2)}(r) \\
&= -\frac{1}{6} D_{1111}^{(2)}(r) - \frac{2}{3r} [D_{1111}(r) - 3D_{11\alpha\alpha}(r)]^{(1)} \\
&\quad - \frac{2}{3r^2} [D_{1111}(r) + 2D_{\beta\beta\beta\beta}(r) - 9D_{11\alpha\alpha}(r)] \\
&\quad + \frac{4}{3} \int_r^\infty y^{-3} [D_{1111}(y) + D_{\beta\beta\beta\beta}(y) \\
&\quad - 6D_{11\alpha\alpha}(y)] dy. \tag{8b}
\end{aligned}$$

The appearance of subscripts  $\alpha$ ,  $\beta$ , and  $\gamma$  in Eq. (8a) emphasizes that use of 2 or 3 for any of these subscripts is arbitrary. For  $r=0$ , both components are  $\chi/3$ , where  $\chi$  is the mean-squared pressure gradient given by [9]

$$\begin{aligned}
\chi &\equiv \frac{1}{\rho^2} \langle |\partial_i P|^2 \rangle = 4 \int_0^\infty r^{-3} [D_{1111}(r) + D_{\beta\beta\beta\beta}(r) \\
&\quad - 6D_{11\gamma\gamma}(r)] dr. \tag{9}
\end{aligned}$$

Of course,  $A_{ij}(\vec{r})$  has the isotropic formula (5), and is therefore described in terms of two scalar functions that are taken to be  $A_{11}(r)$  and  $A_{\gamma\gamma}(r)$ . Because the curl of the gradient is zero, the curl of  $A_{ij}(\vec{r})$  vanishes (operating on either index); consequently, the two scalar functions are related by [Eq. (12.70) of Ref. [4]]

$$A_{11}(r) = A_{\gamma\gamma}(r) + rA_{\gamma\gamma}^{(1)}(r). \tag{10}$$

Thus,  $A_{ij}(\vec{r})$  is described by a single scalar function. Equations (8a) and (8b) satisfy Eq. (10).

The wind-tunnel grid-turbulence velocity data are described in the Appendix. The fourth-order structure functions were calculated from the data and substituted into Eqs. (8a) and (8b). The resulting acceleration correlations are shown in Fig. 1. The single measured transverse velocity component is assigned the subscript 2. The data do not have sufficient spatial resolution to determine  $\chi$  from Eq. (9). In fact, the values shown in Fig. 1 at  $r \leq 2$  mm should be interpreted with caution because of the limited spatial resolution (see the Appendix). The values at  $r=0$  are therefore not graphed in Fig. 1. For  $r=0$ , it is easiest to evaluate Eq. (9) rather than Eqs. (8a) and (8b) from which  $\chi/3$  is the value of  $A_{11}(0)$  and  $A_{\gamma\gamma}(0)$ .

The monotonic decrease of  $A_{22}(r)$  in Fig. 1 is expected [9] on the basis of the monotonic increase of  $D_P^{(1)}(r)$ . Equation (10) requires that  $A_{11}(r)$  have both positive and negative

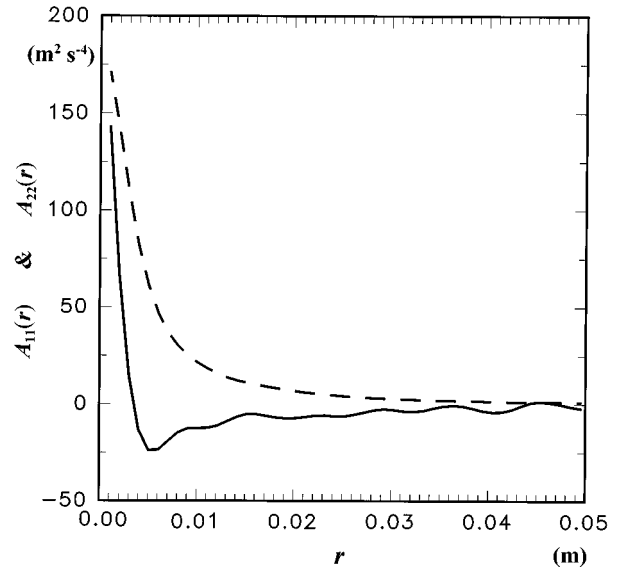


FIG. 1. The acceleration correlation caused by the pressure gradient.  $A_{11}(r)$  and  $A_{22}(r)$  are the solid and dashed curves, respectively. No value is graphed at  $r=0$ . The Kolmogorov microscale was 0.31 mm for this and subsequent figures.

values and therefore have at least 2 extrema [15]. The experimental evaluation shown in Fig. 1 demonstrates that  $A_{11}(r)$  does indeed have a minimum where it is negative. That is, the acceleration components along the separation vector typically have opposite signs for those  $r$  for which  $A_{11}(r)$  is negative. Consider the collision of oppositely directed jets. The acceleration is away from the stall point along the direction of collision and also away from the stall point in the directions transverse to the direction of collision. Such oppositely directed accelerations make it clear that negative values of  $A_{11}(r)$  are expected. In Fig. 1, the minimum value of  $A_{11}(r)$  is about  $-25 \text{ m}^2 \text{ s}^{-4}$ , the square root of the magnitude of which gives relative acceleration of about on-half that of the acceleration of gravity,  $g$ . The minimum occurs at spacings of 5–6 mm and corresponds to  $r/\eta$  about 16–19, where  $\eta$  is Kolmogorov's microscale. The slight oscillations in  $A_{11}(r)$  at the larger  $r$  values shown in Fig. 1 are caused by the limited number of data averaged combined with the cancellations of some of the terms in Eq. (8b). Thus, these oscillations are an artifact that would be removed if much more data were averaged.

In the inertial range, both  $A_{11}(r)$  and  $A_{22}(r)$  are positive and have approximate  $-2/3$  power laws [3,9]. Thus, for an inertial range,  $A_{11}(r)$  must cross zero to become positive at some value of  $r$  [9]. The data do not have an inertial range (see the Appendix), so we do not require another zero crossing of  $A_{11}(r)$  to appear at large  $r$  in Fig. 1.

From the assumption of joint Gaussian velocities, the pressure-gradient contribution to acceleration correlation is [16]

$$A_{\gamma\gamma}^{\text{JG}}(r) = \int_r^\infty y^{-1} [D_{11}^{(1)}(y)]^2 dy, \tag{11a}$$

$$A_{11}^{\text{JG}}(r) = A_{\gamma\gamma}^{\text{JG}}(r) - [D_{11}^{(1)}(r)]^2. \tag{11b}$$

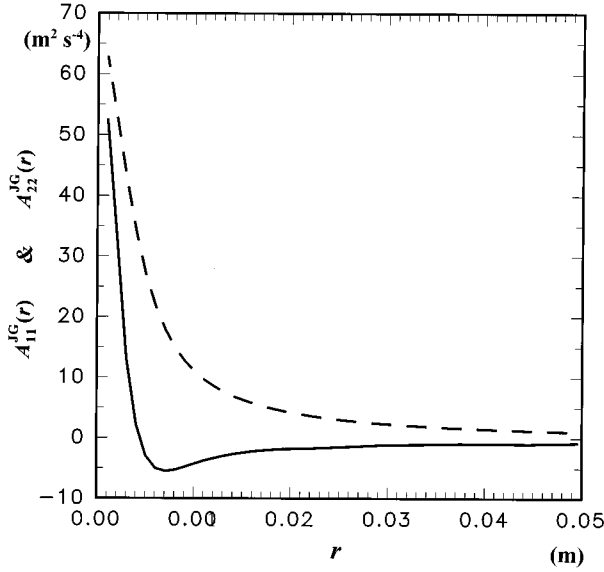


FIG. 2. The acceleration correlation caused by the pressure gradient for the assumption of joint Gaussian velocities.  $A_{11}^{JG}(r)$  and  $A_{22}^{JG}(r)$  are the solid and dashed curves, respectively. No value is graphed at  $r=0$ .

The superscript JG indicates that the formula requires the assumption of joint Gaussian velocities in addition to requiring the postulates. Equations (11a) and (11b) are much simpler than the corresponding formulas in Ref. [3] because integration by parts was not used to simplify the results of Ref. [3]. For comparison with the results in Fig. 1, Eqs. (11a) and (11b) are evaluated using the data, and the pressure-gradient's acceleration correlation is shown in Fig. 2. Results in Fig. 2 appear to be similar to those in Fig. 1. However, note that the scale of the ordinate in Fig. 2 is about one-third that of Fig. 1. That is, the joint Gaussian velocities assumption underestimates the acceleration correlation for the subject data by about a factor of 3. Such an underestimate was anticipated [9]. The minimum of  $A_{11}^{JG}(r)$  in Fig. 2 is at slightly greater  $r$  than in Fig. 1, and the minimum value of  $A_{11}^{JG}(r)$  is almost one-fifth that of  $A_{11}(r)$ .

One can express the acceleration correlations in terms of spectra. Substituting the relationships (8a) and (8b), i.e.,  $A_{\gamma\gamma}(r) = (1/2r)D_p^{(1)}(r)$  and  $A_{11}(r) = (1/2)D_p^{(2)}(r)$ , into Eqs. (15) and (44) of Ref. [9], one immediately relates the Fourier transforms of  $A_{\gamma\gamma}(r)$  and  $A_{11}(r)$  to the pressure spectrum. The pressure spectrum is, in turn, related to the fourth-order velocity structure function [cf. Eq. (16) of Ref. [9]].

### III. ACCELERATION BY THE VISCOUS FORCE

The formula for the viscous acceleration correlation is [3,4]

$$V_{ij}(\vec{r}) \equiv \nu^2 \langle \nabla^2 u_i \nabla'^2 u'_j \rangle = -\frac{\nu^2}{2} D_{ij}(\vec{r})|_{nnkk}. \quad (12)$$

The repeated Roman subscripts following the vertical bar mean that the Laplacian operator with respect to  $\vec{r}$  operates twice on the right-hand side of Eq. (12). Of course,  $V_{ij}(\vec{r})$  obeys the isotropic formula (5), as does  $D_{ij}(\vec{r})$ . In addition,

the divergence of Eq. (12), operating on either index, vanishes because of incompressibility such that  $D_{ij}(\vec{r})|_i = D_{ij}(\vec{r})|_j = 0$ , and therefore,  $V_{ij}(\vec{r})|_i = V_{ij}(\vec{r})|_j = 0$ . That is,  $D_{ij}(\vec{r})$  and  $V_{ij}(\vec{r})$  are both solenoidal such that their components are related by [4]

$$V_{\gamma\gamma}(r) = V_{11}(r) + \frac{r}{2} V_{11}^{(1)}(r); \quad (13)$$

the analogous relationship between  $D_{11}(r)$  and  $D_{\gamma\gamma}(r)$  is well known [4]. Now, Eq. (13) requires that  $V_{\gamma\gamma}(r)$  has both positive and negative values and therefore has at least 2 extrema at finite  $r$  [15].

On the basis of the postulates, Obukhov and Yaglom [3] used Eq. (12) to derive the viscous acceleration correlation in terms of  $D_{11}(r)$ . Unfortunately, substituting data into their formula is not useful for two reasons. First, that formula requires derivatives of first through fifth order of  $D_{11}(r)$  with respect to  $r$ , or derivatives of up to fourth order if both  $D_{22}(r)$  and  $D_{11}(r)$  appear in the formula. Second, their result vanishes when the asymptotic viscous-range formula,  $D_{11}(r) \propto r^2$ , is substituted into their formula; this implies great cancellation of terms in the formula for  $r$  within the viscous range, whereas the viscous range is the most significant range for viscous acceleration correlation. Indeed, the second property is the reason that fourth-order derivative moments appear in the formulas for the mean-squared viscous acceleration given by Batchelor [5] and Yaglom [6].

Therefore, another formula is sought that does not have these properties. Monin [17] was the first to obtain, on the basis of the postulates, that

$$D_{ijk}(\vec{r})|_k + \frac{4}{3} \epsilon \delta_{ij} = 2\nu D_{ij}(\vec{r})|_{kk} \quad (14)$$

[cf. Eq. (22.15) in Ref. [4]], from which follows Kolmogorov's equation [4,17,18]

$$D_{111}(r) = -\frac{4}{5} \epsilon r + 6\nu D_{11}^{(1)}(r), \quad (15)$$

where  $\epsilon$  is the rate of dissipation of turbulent energy per unit mass of fluid. Applying the Laplacian operator to Eq. (14) gives

$$D_{ijk}(\vec{r})|_{knn} = 2\nu D_{ij}(\vec{r})|_{nnkk}. \quad (16)$$

Substituting Eq. (16) into Eq. (12) gives

$$V_{ij}(\vec{r}) = -\frac{\nu}{4} D_{ijk}(\vec{r})|_{knn}. \quad (17)$$

The longitudinal and transverse components of the viscous acceleration correlation are obtained by substitution of the isotropic formula for  $D_{ijk}(\vec{r})$  and use of incompressibility [Eq. (6)], as follows:

$$V_{\gamma\gamma}(r) = \frac{\nu}{2} \left[ \frac{1}{r^3} D_{111}(r) + \frac{2}{r^3} D_{1\beta\beta}(r) - \frac{5}{r^2} D_{1\beta\beta}^{(1)}(r) - \frac{1}{r} D_{1\beta\beta}^{(2)}(r) \right], \quad (18a)$$

$$V_{11}(r) = \frac{\nu}{2} \left[ -\frac{1}{r^3} D_{111}(r) + \frac{2}{r^3} D_{1\beta\beta}(r) + \frac{1}{r^2} D_{1\beta\beta}^{(1)}(r) - \frac{3}{r} D_{1\beta\beta}^{(2)}(r) - \frac{1}{2} D_{1\beta\beta}^{(3)}(r) \right]. \quad (18b)$$

Of course, Eq. (6) can be used to express  $V_{\gamma\gamma}(r)$  and  $V_{11}(r)$  in terms of only  $D_{111}(r)$ ; a one-order-higher derivative would then appear in these formulas, and more cancellation among the terms would occur. Equations (18a) and (18b) have been checked by determining that they agree with the expression for  $V_{ii}(0)$  given by Yaglom [6] and that they produce the same inertial-range formula for viscous acceleration correlation as can be obtained from the formulas in Ref. [3]. Also, Eqs. (18a) and (18b) obey the incompressibility condition [Eq. (13)].

From Eqs. (18a) and (18b), the asymptotic viscous-range formulas are

$$V_{11}(0) = V_{\gamma\gamma}(0) = -35\nu\langle(\partial_1 u_1)^3\rangle/6, \quad (19)$$

which is the same as obtained by Yaglom [6], who used a different method.

Derivation of the inertial-range formulas from Eqs. (18a) and (18b) is given next. If the isotropic formula for  $D_{ijk}(\vec{r})$  and Kolmogorov's [18] inertial-range law, i.e.,  $D_{111}(r) = -4\epsilon r/5$  and  $D_{1\gamma\gamma}(r) = -4\epsilon r/15$ , are substituted on the left-hand side of Eq. (16), then the left-hand side of Eq. (16) vanishes. The inertial-range law is thus the solution to the corresponding homogeneous equation [i.e., replacing the right-hand side of Eq. (16) with zero]. Therefore, the correction to the inertial-range formula for  $D_{111}(r)$  can be found by substituting the inertial-range formula for  $D_{ij}(\vec{r})$  on the right-hand side of Eq. (16) and obtaining the particular solution of Eq. (16). It is simpler to substitute the inertial-range formula  $D_{11}(r) = C\epsilon^{2/3}r^{2/3}$  into Kolmogorov's equation, Eq. (15), and solve for  $D_{111}(r)$  to obtain

$$D_{111}(r) = -\frac{4}{5}\epsilon r + 4\nu C\epsilon^{2/3}r^{-1/3} = -\frac{4}{5}\epsilon r[1 - 5C(r/\eta)^{-4/3}], \quad (20a)$$

$$D_{1\gamma\gamma}(r) = -\frac{4}{15}\epsilon r + \frac{4}{9}\nu C\epsilon^{2/3}r^{-1/3} = -\frac{4}{15}\epsilon r[1 - \frac{5}{3}C(r/\eta)^{4/3}], \quad (20b)$$

where Eq. (20b) follows from Eq. (20a) on the basis of incompressibility [Eq. (6)]. Here,  $\eta = (\nu^3/\epsilon)^{1/4}$  is Kolmogorov's microscale, and  $C$  is Kolmogorov's constant, which has the value  $C \approx 2$  [19]. The result [Eqs. (20a) and (20b)] gives the correction to Kolmogorov's inertial-range law caused by viscous acceleration. The use of  $C=2$  in Eqs. (20a) and (20b) shows that the correction term is small compared to the asymptotic power law for those  $r/\eta$  for which  $D_{11}(r) = C\epsilon^{2/3}r^{2/3}$  is accurate. Substituting Eqs. (20a) and (20b) into Eqs. (18a) and (18b) gives the same result as can be obtained by substituting the inertial-range formula for  $D_{11}(r)$  into the formulas for  $V_{11}(r)$  and  $V_{\gamma\gamma}(r)$  given in Ref. [3]; this fact validates Eqs. (18a) and (18b) and the correction terms in Eqs. (20a) and (20b) because only the correction terms contribute to  $V_{11}(r)$  and  $V_{\gamma\gamma}(r)$ . The inertial-range asymptotic formulas arise only from the correction terms in Eqs. (20a) and (20b) and are

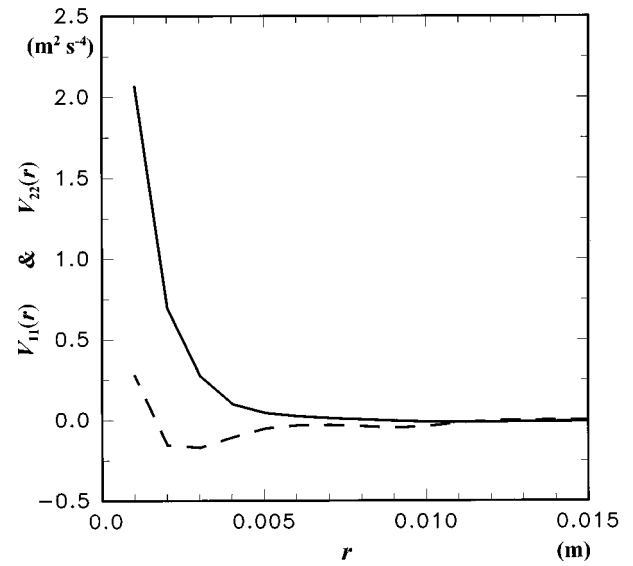


FIG. 3. The acceleration correlation caused by the viscous force.  $V_{11}(r)$  and  $V_{22}(r)$  are the solid and dashed curves, respectively. No value is graphed at  $r=0$ .

$$V_{11}(r) = 2.72\nu^2 C\epsilon^{2/3}r^{-10/3}, \quad (21a)$$

$$V_{\gamma\gamma}(r) = -1.84\nu^2 C\epsilon^{2/3}r^{-10/3}. \quad (21b)$$

The  $-10/3$  power law has been given by Obukhov and Yaglom [3]. Since only the correction terms in Eqs. (20a) and (20b) contribute in Eqs. (21a) and (21b), it follows that if one were to attempt to use data to calculate  $V_{11}(r)$  and  $V_{\gamma\gamma}(r)$  in the inertial range, then one should use their relationship to  $D_{11}(r)$  given in Ref. [3] rather than use Eqs. (18a) and (18b). On the other hand, Eqs. (18a) and (18b) should be used for the viscous range for aforementioned reasons.

The third-order structure functions were calculated from the data and substituted into Eqs. (18a) and (18b). The result is shown in Fig. 3. The negative values of  $V_{22}(r)$ , which are required on the basis of Eq. (13) [15], are evident in Fig. 3. Note that the scale of the abscissa in Fig. 3 is less than one-third that of Figs. 1 and 2, and that the scale of the ordinate in Fig. 3 is only about one-hundredth that of Fig. 1. The evaluation shown in Fig. 3 clearly suffers from limited spatial resolution of the data to a greater extent than the pressure-gradient correlation in Fig. 1. Evaluation of Eq. (19) gives  $2.7 \text{ m}^2 \text{ s}^{-4}$  (see the Appendix), which is greater than the values graphed in Fig. 3 at the minimum spacing of 1 mm especially for  $A_{22}(r)$ . This indicates that the derivatives in Eqs. (18a) and (18b) are inaccurate at the smallest spacing in Fig. 3 because of the limited spatial resolution of the data and the coarseness of the sampling rate, especially when it is necessary to calculate the third-order derivative, as in Eq. (18b). The viscous acceleration correlation was also calculated from  $D_{111}(r)$  alone; that is, by calculating the right-hand side of Eq. (6) and using it in place of  $D_{1\beta\beta}(r)$  everywhere in Eqs. (18a) and (18b). The result differed from Fig. 3 in only minor respects; notably, there were more oscillations at the larger  $r$  caused by the higher order of differentiation.

Fourier transformation of Eqs. (18a) and (18b) followed by integration by parts and optional use of Eq. (6), can be used to express the Fourier transforms of  $V_{\gamma\gamma}(r)$  and  $V_{11}(r)$  in terms of Fourier transforms related to  $D_{111}(r)$  and  $D_{1\beta\beta}(r)$ . Alternatively, the Fourier transforms of the relationships of  $V_{\gamma\gamma}(r)$  and  $V_{11}(r)$  to  $D_{111}(r)$  as given in Ref. [3] can, after integration by parts, express the Fourier transforms of  $V_{\gamma\gamma}(r)$  and  $V_{11}(r)$  in terms of Fourier transforms that involve  $D_{11}(r)$ .

#### IV. DISCUSSION

The contributions of the pressure gradient and the viscous force to the fluid-particle acceleration correlation were evaluated using velocity data. It appears that spatial resolution on the order of the Kolmogorov microscale is needed to better obtain the acceleration caused by the viscous force. Achieving such fine spatial resolution requires considerable experimental effort. About half that resolution is needed for the pressure-gradient correlation. Data that is sampled more finely than the spatial resolution would be useful for implementing the derivatives. Much more data than that used here would improve the statistical reliability and thereby improve evaluation of the correlations. A motivation for this report is to encourage the design of experiments capable of evaluating the acceleration correlation.

The asymptotic formulas for  $V_{ij}(\vec{r})$  in the viscous and inertial ranges are given in Eqs. (19), (20a), and (20b) and for  $A_{ij}(\vec{r})$  in Ref. [9]. The data employed cannot be used to verify either asymptote. For simplicity, the inertial-range power laws are given without their modifications attributable to intermittency, but the modification is obvious.

All results are obtained solely on the basis of the postulates, with the exception, of course, of the inertial-range asymptotic formulas [Eqs. (20b), (21a), and (21b)] and the comparison with results from the joint Gaussian assumption. Results based solely on the postulates are valid for arbitrary Re. In practice, as Re becomes small, the turbulence must become homogeneous and isotropic in order that local homogeneity and local isotropy remain accurate. Numerical simulation of turbulence can be used to calculate both sides of Eqs. (8a) and (8b) and Eqs. (18a) and (18b). As such, these equations and related equations in Ref. [9] can be used as measures of how well the simulation obeys the postulates. Equations (8a) and (8b) and related equations in Ref. [9] do not depend on the viscosity term; thus, these equations are satisfied when hyperviscosity is used in a numerical simulation, as in Ref. [2].

Figure 1 shows that the transverse component caused by the pressure gradient, i.e.,  $A_{\gamma\gamma}(r)$ , is monotonically decreasing, as expected, and that the longitudinal component, i.e.,  $A_{11}(r)$ , has a minimum where it is negative. The latter implies that accelerations at the two points are, in the root-mean-squared sense, toward and away from each other when projected on the separation vector  $\vec{r}$ . The maximum contributions to the acceleration correlation are at  $r=0$ , where, for the data considered, the pressure gradient contributes a value in excess of  $175 \text{ m}^2 \text{ s}^{-4}$  (thus, the root-mean-squared acceleration exceeds 1.4 g) and the viscous force contributes  $2.7 \text{ m}^2 \text{ s}^{-4}$ . At all  $r$ , the viscous-force contribution is small compared with that of the pressure gradient, and it is even

smaller, relative to the pressure-gradient contribution, for even greater Re. The assumption of joint Gaussian velocities causes underestimation of the pressure-gradient correlation by about a factor of 3 for the data considered, and the underestimate worsens with increasing Re.

#### ACKNOWLEDGMENTS

The authors thank W. T. Otto for assistance with the computation. This work was partially supported by ONR Contract No. N00014-93-F-0038.

#### APPENDIX

Velocity data obtained from grid-generated turbulence in a wind tunnel were used to evaluate Eqs. (8a), (8b), (11a), (11b), (18a), (18b), and (19). The data are described in Ref. [20]. An X-configuration hot-wire anemometer measured the streamwise velocity component, as well as one cross-stream velocity component. These components are assigned the subscripts 1 and 2, respectively, i.e.,  $\beta=\gamma=2$ . The grid spacing was 19 cm. The measurements were performed 4.7 m from the grid, at which position the mean shear was zero. The mean velocity was  $10.1 \text{ m s}^{-1}$ , the Kolmogorov microscale  $\eta$  was 0.31 mm. Taylor's scale was 8.5 mm, the integral scale was 10.8 cm [20], and  $\text{Re}=208$ . The hot wires were 1.2 mm long, and the signals were filtered at 5 kHz, so the spatial scale over which the velocity was averaged was about 1 mm. The data were sampled at 10 kHz, so using Taylor's hypothesis with the mean velocity of  $10.1 \text{ m s}^{-1}$ , the samples were spaced 1 mm in the streamwise direction. Reduced credibility must be given to the statistics at spacings less than about 2 mm because of the spatial averaging.

The statistical reliability of the structure functions was determined by calculating joint probability distributions and graphing the integrands that produce the statistics by integration of a function multiplying the joint probability distribution. For instance, the integrand for  $D_{1122}(r)$  at a given  $r$  is  $(u_1 - u'_1)^2(u_2 - u'_2)^2$  times the joint probability distribution of  $(u_1 - u'_1)$  and  $(u_2 - u'_2)$ . There is no systematic underestimation of any of the statistics.

The velocity structure functions were corrected for inaccuracy of Taylor's frozen-flow hypothesis using the algorithms in Ref. [21]. Those algorithms include corrections for second-, third-, and fourth-order structure functions. Unnoticeable changes in the figures results from using corrected versus uncorrected structure functions.

The velocity covariances were  $\langle(u_1)^2\rangle=0.135 \text{ m}^2 \text{ s}^{-2}$ ,  $\langle(u_2)^2\rangle=0.119 \text{ m}^2 \text{ s}^{-2}$ , and  $\langle u_1 u_2 \rangle = -0.0036 \text{ m}^2 \text{ s}^{-2}$ , which show that the turbulence was nearly isotropic. The numerators of the ratios  $D_{12}(r)/D_{11}(r)$ ,  $D_{1112}(r)/D_{1111}(r)$ , and  $D_{1222}(r)/D_{1111}(r)$  should be zero in isotropic turbulence. These ratios were within 2% of zero for  $r<10$  cm with the exception of a rapid decrease for  $r<0.3$  cm, presumably caused by spatial averaging and the separation of the two wires in the X-wire probe.

The power spectra of both velocity components have power laws extending over about a decade in wave number [20], but the power-law exponents are noticeably shallower than  $-5/3$ ; they are about  $-5/3+0.19$ . This deviation from  $-5/3$  is expected for the Reynolds number of 208 in com-

parison with slopes of velocity spectra collected in the fifth figure of Ref. [22], and in comparison with the dissipation range bump observed in velocity spectra at higher Reynolds numbers [1,23–25] and predicted theoretically [26,27].

A finite value must be chosen for the upper limit of the integral in Eq. (8a). The integrand in Eq. (8a), as evaluated using the data, decreases in a nearly power-law manner by more than 3 decreases from  $r=5$  mm to 9 cm; beyond 10 cm, the integrand becomes statistically unreliable. The upper limit was chosen to be 10 cm. Because of the rapid decrease

of the integrand with increasing  $r$ , the integral is insensitive to the choice of the upper limit. Similar considerations establish 20 cm as the appropriate upper limit for use in Eqs. (11a) and (11b).

For  $r=1$  mm, i.e., the minimum spacing, the ratio  $D_{111}(r)/[D_{11}(r)]^{3/2}$  was  $-0.4$ , which agrees with the value of velocity-derivative skewness given for the same data in Ref. [20]. This value was used with Eq. (19) and the measured energy dissipation rate to obtain  $V_{11}(0)=V_{\gamma\gamma}(0)=2.7 \text{ m}^2 \text{ s}^{-4}$ .

- 
- [1] S. G. Saddoughi and S. V. Veeravalli, *J. Fluid Mech.* **268**, 333 (1994).
- [2] V. Borue and S. A. Orszag, *J. Fluid Mech.* **306**, 293 (1996).
- [3] A. M. Obukhov and A. M. Yaglom, *Prikl. Mat. Mekh.* **15**, 3 (1951) [translation in National Advisory Committee for Aeronautics (NACA), TM 1350, Washington, DC (1953)].
- [4] A. S. Monin and A. M. Yaglom, *Statistical Fluid Mechanics: Mechanics of Turbulence* (MIT Press, Cambridge, 1975), Vol. 2.
- [5] G. K. Batchelor, *Proc. Cambridge Philos. Soc.* **47**, 359 (1951).
- [6] A. M. Yaglom, *Dok. Akad. Nauk SSSR* **67**, 795 (1949).
- [7] O. Métais and M. Lesieur, *J. Fluid. Mech.* **239**, 157 (1992).
- [8] A. Pumir, *Phys. Fluids* **6**, 2071 (1994).
- [9] R. J. Hill and J. M. Wilczak, *J. Fluid Mech.* **296**, 247 (1995).
- [10] C. C. Lin, *Quart. Appl. Math.* **X**, 295 (1953).
- [11] H. Chen, J. R. Herring, R. M. Kerr, and R. H. Kraichnan, *Phys. Fluids A* **1**, 1844 (1989).
- [12] G. Münch and A. D. Wheelon, *Phys. Fluids* **1**, 462 (1958).
- [13] H. Tennekes, *J. Fluid Mech.* **67**, 561 (1975).
- [14] G. Heskestad, *J. Appl. Mech.* **87**, 735 (1965).
- [15] See the discussion in Ref. [4] following their Eq. (12.82). For the requirement that  $A_{11}(r)$  and  $V_{\gamma\gamma}(r)$  have both positive and negative values, one must require that, as  $r \rightarrow \infty$ ,  $A_{\gamma\gamma}(r)$  and  $V_{11}(r)$  approach zero more rapidly than  $r^{-1}$  and  $r^{-2}$ , respectively.
- [16] R. J. Hill, National Oceanic and Atmospheric Administration (NOAA) Technical Report No. ERL 451-ETL 66, 1994 (available from the author or the National Technical Information Service, 5285 Port Royal Rd., Springfield, VA 22161).
- [17] A. S. Monin, *Dok. Akad. Nauk SSSR* **125**, 515 (1959).
- [18] A. N. Kolmogorov, *Dok. Akad. Nauk SSSR* **32**, 19 (1941).
- [19] A. M. Yaglom, *Izv. Acad. Sci. USSR, Atmos. Oceanic Phys.* **17**, 919 (1981).
- [20] S. T. Thoroddsen, *Phys. Fluids* **7**, 691 (1995).
- [21] R. J. Hill, *Atmos. Res.* **40**, 153 (1996).
- [22] K. R. Sreenivasan, *Phys. Fluids* **8**, 189 (1996).
- [23] F. H. Champagne, C. A. Friehe, J. C. La Rue, and J. C. Wyngaard, *J. Atmos. Sci.* **34**, 515 (1977).
- [24] R. M. Williams and C. A. Paulson, *J. Fluid Mech.* **83**, 547 (1977).
- [25] P. Mestayer, *J. Fluid Mech.* **125**, 475 (1982).
- [26] G. Falkovich, *Phys. Fluids* **6**, 1411 (1994).
- [27] D. Lohse and A. Müller-Groeling, *Phys. Rev. Lett.* **74**, 1747 (1995).